

**ELECTROLESS COPPER COMPOSITE
COATINGS REINFORCED WITH SILICON
CARBIDE AND GRAPHITE PARTICLES**

SOHEILA FARAJI

UNIVERSITI SAINS MALAYSIA

2011

**ELECTROLESS COPPER COMPOSITE COATINGS
REINFORCED WITH SILICON CARBIDE AND
GRAPHITE PARTICLES**

By

SOHEILA FARAJI

Thesis submitted in fulfillment of the requirements
for the degree of Doctor of Philosophy

JULY 2011

DEDICATION

This present thesis is dedicated to my beloved mom and dad who are my
true sources of life and love

Thank you and I love you

SOHEILA

In every job that you are professional and not let the pessimism of barren and not let that get infected with some regrettable moments for any nation that comes before you pull the hopelessness and despair. Peace prevailing in laboratories and libraries backed Live. First ask yourself: "I've been learning how to? As earlier, then go to ask: What I've been to my country? And these questions continue to do so to feel joyful and exciting, which can become: "Maybe a small share and promote the advancement of humanity have had. But regardless of any reward save that life or not to give to our efforts, then the moment of death comes upon each of us should have the right to say that out loud "I've had what could have done".

Loyi Pastor

ACKNOWLEDGEMENTS

Now, finishing this phase of study (Ph.D.), I am so pleased to express some words which are different to say directly.

First of all, I thank Allah for bestowing health upon me to be able to think and for paving the way to gain further knowledge. I had never thought of coming to Malaysia for continuing my study; however it was my destiny to come to this country which brought me great blessings. It was actually a wonderful experience for me in acquiring academic advances and learning how to think appropriately, be patient, do my best effort, practice resistance, gain cognition and humility and above all give love to all fellow human beings. It is not an overstatement to say this stage was the best evolution I have ever made in my life. Thanks to Allah, then I am indebted to generous, honest and kind people of Malaysia.

There are many people that I would like to express my deepest gratitude for their support along the way. Above all, I wish to express sincere thanks to my main supervisor, Dr. Afidah Abdul Rahim (Deputy Dean of Academic & Student Affairs of the School of Chemical Sciences), for her valuable guidance, motivation, patience, and supports throughout the completion of this work both intellectually and financially. I am proud that I am her first Ph.D. student.

I wish to extend special thanks to my main co-supervisor, Prof. Norita Mohamed (Deputy Dean of Research & Postgraduate of the School of Chemical Sciences), for her advice, assistance, encouragement and support during the progress of this research.

I am so grateful to my second co-supervisor, Assoc. Prof. Coswald Stephen Sipaut @ Mohd. Nasri, Universiti Malaysia Sabah (since July 2009), for his advice and assistance of this research.

I would like to acknowledge Universiti Sains Malaysia (USM), honorable Vice Chancellor and all the academic staff, technical staff, other faculty members

and staffs of the School of Chemical Sciences for providing me with all the facilities during my studies. Special thanks also extended to Assoc. Prof. Mohd Jain Kassim who has kindly let me use his lab.

Here I also wish to extend my acknowledgements to honorable Dean of the School of Chemical Sciences Prof. Wan Ahmad Kamil and Prof. Bahruddin Saad as ex- Deputy Dean of Research & Postgraduate studies of the School of Chemical Sciences.

I would like to express my special thanks to the Institute of Graduate Studies (IPS) for offering a PRGS (Postgraduate Research Grant Scheme) on my project. I would also like to thank Malaysian Ministry of Higher Education for supplying the financial assistance for this research through RU (Research University) grant to me.

I wish to express my special gratitude to all other faculty members and staffs of the EM-unit School of Biological Sciences and XRD and AFM units at School of Physical Science and Mechanical-units of Material Engineering School and Technical Center and library and International House of USM for their tremendous help and kind assistance. I would also like to specially thanks Universite Henri Poincare (UHP), France for the use of their SEM facilities.

I wish to express my greatest thanks to our research group members for their valuable suggestion, discussion and kindness and to all my lovely friends.

Last but not the least, I owe my deepest gratitude to all my lovely family members: my father, mother, sisters (Mitra & Maryam), brother (Amir Hossein) and my two dear sweet nephews (Amir Ahmad & Amir Hesam) for their extremely encouragement and great spiritual support in my goal of completing this study.

Thank you very much everyone for your unceasing encouragement, that have made this dream comes true.

Soheila Faraji

2011

TABLE OF CONTENTS

	<i>Page</i>
ACKNOWLEDGEMENTS	iii
TABLE OF CONTENTS	v
LIST OF TABLES	xi
LIST OF FIGURES	xiv
LIST OF ABBREVIATIONS	xxii
ABSTRAK	xxiv
ABSTRACT	xxvi
CHAPTER ONE - INTRODUCTION & LITERATURE REVIEWS	1
1.1 Electroless plating	1
1.2 General process and bath composition	4
1.3 Electroless copper (EC) and functional applications	8
1.4 Carbon steel (CS)	12
1.5 Composite coating	14
1.5.1 Reinforcement of coatings by silicon carbide	17
1.5.2 Reinforcement of coatings by graphite (C _g)	21
1.6 Corrosion	22
1.6.1 Fundamentals	22
1.6.2 Why Metals Corrode	22
1.6.3 Corrosion Measurements	23
1.6.3.1 Potentiodynamic polarisation	24

1.6.3.2	Electrochemical Impedance Spectroscopy (EIS)	28
1.7	Tribological and mechanical behaviours	34
1.7.1	Wear and friction coefficient	34
1.7.2	Hardness	36
1.8	Problem, scope, objectives and organization of the thesis	38
1.8.1	Problem statement	38
1.8.2	Scope	40
1.8.3	Objectives	40
1.8.4	Organization of the thesis	41
	CHAPTER TWO - MATERIALS AND METHODS	42
2.1	Electroless plating of composite coatings	42
2.1.1	The pretreatment of carbon steel substrates	42
2.1.2	Optimisation of composite coatings	42
2.2	Surface analysis	44
2.2.1	Scanning Electron Microscopy (SEM) with Energy Dispersive X-ray spectroscopy (EDX)	44
2.2.2	X-ray diffraction (XRD)	44
2.2.3	Differential Scanning Calorimetry (DSC)	45
2.2.4	Atomic Force Microscopy (AFM)	46
2.3	Corrosion rate measurements	46
2.3.1	Weight loss technique	46
2.3.2	Potentiodynamic polarisation studies	47
2.3.3	Electrochemical Impedance Spectroscopy (EIS) studies	49
2.4	Tribological and mechanical behaviours	50
2.4.1	Microhardness test	50

2.4.2	Wear test and friction coefficient	50
CHAPTER THREE - RESULTS AND DISCUSSION		51
3.1	Optimisation and characterisation of the Cu–P, Cu–P–SiC, Cu–P–C _g and Cu–P–C _g –SiC composite coatings	51
3.1.1	SEM analysis of carbon steel substrate	51
3.1.2	Electroless Cu–P composite coating on carbon steel substrate	52
3.1.3	Optimisation of electroless Cu–P–SiC composite coating on carbon steel substrate	54
3.1.3.1	Effect of NaH ₂ PO ₂ ·H ₂ O concentration on deposition rate and composition of coatings	54
3.1.3.2	Effect of temperature on deposition rate and composition of coatings	56
3.1.3.3	Effect of pH on deposition rate and composition of coatings	57
3.1.3.4	Effect of NiSO ₄ ·6H ₂ O concentration on deposition rate and composition of coatings	59
3.1.3.5	Effect of SiC concentration on deposition rate and composition of coatings	61
3.1.3.6	Effect of sodium citrate concentration on deposition rate and composition of coatings	63
3.1.3.7	Effect of H ₃ BO ₃ concentration on deposition rate and composition of coatings	65
3.1.3.8	Surface analysis of electroless Cu–P–SiC by SEM and EDX	66
3.1.4	Optimisation of electroless Cu–P–C _g composite coating on carbon steel substrate	68
3.1.4.1	Effect of C _g concentration on deposition rate and composition of coatings	68
3.1.4.2	Surface analysis of electroless Cu–P–C _g by SEM and EDX	70

3.1.4.3	Surface analysis of electroless Cu–P–C _g –SiC by SEM and EDX	73
3.1.5	XRD analysis of composite coatings	75
3.1.6	DSC analysis of composite coatings	81
3.2	Corrosion studies	86
3.2.1	Weight loss method	87
3.2.1.1	The effect of SiC content on corrosion resistance of Cu–P–SiC composite coating in 3.5 % NaCl and 1 M HCl solutions	87
3.2.1.2	The comparison of corrosion behaviour of electroless Cu–P, Cu–P–SiC, Cu–P–C _g , Cu–P–C _g –SiC composite coatings in 3.5 % NaCl and 1 M HCl solutions	89
3.2.1.3	The study of Cu–P and Cu–P–SiC composite coatings in 3.5 %, 10 %, 20 % NaCl, 0.1 M, 0.5 M and 1 M HCl solutions	91
3.2.2	Corrosion studies by the potentiodynamic polarisation	96
3.2.2.1	The effect of different SiC concentrations on the corrosion rate of Cu–P–SiC on carbon steel in the 3.5 % NaCl and 1 M HCl solutions	97
3.2.2.2	The comparison of corrosion behaviour of electroless Cu–P, Cu–P–SiC, Cu–P–C _g , Cu–P–C _g –SiC composite coatings in 3.5 % NaCl and 1 M HCl solutions	100
3.2.2.3	The study of Cu–P and Cu–P–SiC composite coatings in 3.5 %, 10 %, 20 % NaCl, 0.1 M, 0.5 M and 1 M HCl solutions	107
3.2.3	Corrosion studies by Electrochemical Impedance Spectroscopy (EIS)	112
3.2.3.1	The effect of different SiC concentrations on	113

	the corrosion rate of Cu-P-SiC on carbon steel in the 3.5 % NaCl solution	
3.2.3.2	The comparison of corrosion behaviour of electroless of Cu-P, Cu-P-SiC, Cu-P-C _g and Cu-P-C _g -SiC composite coatings in 3.5 % NaCl solution	118
3.2.3.3	The effect of different SiC concentrations on the corrosion rate of Cu-P-SiC on carbon steel in 1 M HCl solutions	123
3.2.3.4	The comparison of corrosion behaviour of electroless of Cu-P, Cu-P-SiC, Cu-P-C _g and Cu-P-C _g -SiC composite coatings in 1 M HCl solution	127
3.3	Mechanical and tribological behaviour studies	132
3.3.1	Microhardness test	133
3.3.1.1	Comparison of microhardness Cu-P, Cu-P-SiC, Cu-P-C _g and Cu-P-C _g -SiC composite coatings	133
3.3.1.2	The effect of SiC content on hardness of Cu-P-SiC composite coating	134
3.3.1.3	The effect of C _g content on hardness of Cu-P-C _g composite coating	135
3.3.2	The wear rate	135
3.3.2.1	Comparison of wear rate of Cu-P, Cu-P-SiC, Cu-P-C _g and Cu-P-C _g -SiC composite coatings	135
3.3.2.2	The effect of SiC content on wear rate of Cu-P-SiC composite coating	137
3.3.2.3	The effect of C _g content on wear resistance of Cu-P-C _g composite coating	138
3.3.2.4	Evaluation of worn surfaces	139
3.3.3	Friction coefficient	142

3.3.3.1	Comparison of the friction coefficient of Cu–P, Cu–P–SiC, Cu–P–C _g and Cu–P–C _g –SiC composite coatings	142
3.3.3.2	The effect of SiC content on friction coefficient of Cu–P–SiC composite coating	145
3.3.3.3	The effect of C _g content on friction coefficient of Cu–P–C _g composite coating	147
3.4	AFM analysis	149
CHAPTER FOUR - CONCLUSIONS		151
4.1	Conclusion	151
4.2	Recommendations for future research	154
REFERENCES		157
APPENDICES		179
LIST OF PUBLICATIONS		188

LIST OF TABLES

		<i>Page</i>
Table 1.1	General electroless bath composition (Delaunois <i>et al.</i> , 2000)	7
Table 2.1	Composition (g L^{-1}) and operating conditions of electroless Cu–P coatings	43
Table 3.1	Composition (g L^{-1}) and operating conditions of electroless Cu–P coating	53
Table 3.2	Composition (g L^{-1}) and operating conditions of electroless Cu–P–SiC coating	67
Table 3.3	Composition (g L^{-1}) and operating conditions of electroless Cu–P–C _g coating	71
Table 3.4	Corrosion characteristics of as plated electroless Cu–P–SiC coatings deposited from the baths with different concentrations of SiC in 3.5 % NaCl	99
Table 3.5	Corrosion characteristics of as plated electroless Cu–P–SiC coatings deposited from the baths with different concentrations of SiC in 1 M HCl on carbon steel substrates	100
Table 3.6	Corrosion characteristics of as plated electroless Cu–P composite coatings and carbon steel substrate in 3.5 % NaCl solution	101
Table 3.7	Corrosion characteristics of as plated electroless Cu–P composite coatings and carbon steel substrate in 1 M HCl solution	102

Table 3.8	Corrosion characteristics of as plated electroless Cu–P, Cu–P–SiC coatings and carbon steel substrate in 3.5 %, 10 % and 20 % NaCl solutions	109
Table 3.9	Corrosion characteristics of as plated electroless Cu–P, Cu–P–SiC coatings and carbon steel substrate in 0.1 M, 0.5 M and 1 M HCl solutions	111
Table 3.10	Corrosion characteristics of as plated electroless Cu–P–SiC with different concentrations of SiC coatings and carbon steel substrate in 3.5 % NaCl solution by electrochemical impedance (EIS) studies	117
Table 3.11	Corrosion characteristics of as plated electroless Cu–P composite coatings and carbon steel substrate in 1 M HCl solution by electrochemical impedance (EIS) studies	121
Table 3.12	Corrosion characteristics of as plated electroless Cu–P–SiC with different concentrations of SiC coatings and carbon steel substrate in 1 M HCl solution by electrochemical impedance (EIS) studies	124
Table 3.13	Corrosion characteristics of as plated electroless Cu–P composite coatings and carbon steel substrate in 1 M HCl solution by electrochemical impedance (EIS) studies	132
Table 3.14	The hardness test values of electroless Cu–P composite coatings	134
Table 3.15	The wear rate values of electroless Cu–P composite coatings	136
Table 3.16	The friction coefficient values of electroless Cu–P	143

composite coatings

Table 3.17	Friction coefficient vs. sliding distance for different SiC concentrations in the bath for Cu-P-SiC composite coatings	145
Table 3.18	Friction coefficient vs. sliding distance for different C_g concentrations in the bath for Cu-P- C_g composite coatings	147
Table 3.19	The roughness values of electroless Cu-P composite coatings	149

LIST OF FIGURES

		<i>Page</i>
Figure 1.1	Equilibrium established at: (a) mixed potential (b) mixed potential- the catalytic power of metal (Delaunois <i>et al.</i> , 2000)	4
Figure 1.2	Catalytic activities of metals at 25 °C with different reducing agents (Delaunois <i>et al.</i> , 2000)	6
Figure 1.3	An example of Tafel curve	26
Figure 1.4	Nyquist plot with impedance vector	30
Figure 1.5	Simple equivalent circuit with one time constant	31
Figure 1.6	Bode plot with one time constant	32
Figure 1.7	The equivalent circuit elements that can be used in the moderate cell model	33
Figure 1.8	(a) Nyquist plot and (b) model of Randles cell	34
Figure 1.9	Schematic view of a ring on disk test (Wu <i>et al.</i> , 2006b)	35
Figure 3.1	SEM micrograph of carbon steel substrate	51
Figure 3.2	As plated Cu–P coating on carbon steel substrate	53
Figure 3.3	(a) SEM and (b) EDX analysis of Cu–P composite coating	54
Figure 3.4	Effect of NaH ₂ PO ₂ ·H ₂ O concentration on deposition rate	55

Figure 3.5	Effect of $\text{NaH}_2\text{PO}_2 \cdot \text{H}_2\text{O}$ concentration on deposit composition	55
Figure 3.6	Effect of temperature on deposition rate	56
Figure 3.7	Effect of temperature on deposit composition	57
Figure 3.8	Effect of pH on deposition rate	58
Figure 3.9	Effect of pH on deposit composition	58
Figure 3.10	Effect of $\text{NiSO}_4 \cdot 6\text{H}_2\text{O}$ concentration on deposition rate	60
Figure 3.11	Effect of $\text{NiSO}_4 \cdot 6\text{H}_2\text{O}$ concentration on deposit composition	60
Figure 3.12	Effect of SiC concentration on deposition rate	62
Figure. 3.13	Effect of SiC concentration on deposit composition	62
Figure. 3.14	The effect of SiC concentration on the particle content in the deposits	63
Figure 3.15	Effect of sodium citrate concentration on deposition rate	64
Figure 3.16	Effect of sodium citrate concentration on deposit composition	64
Figure 3.17	Effect of H_3BO_3 concentration on deposition rate	65
Figure 3.18	Effect of H_3BO_3 concentration on deposit composition	66

Figure 3.19	As plated Cu–P–SiC coating on carbon steel substrate	67
Figure 3.20	(a) SEM and (b) EDX analysis of Cu–P–SiC composite coating	68
Figure 3.21	Effect of C_g concentration on deposition rate	69
Figure 3.22	Effect of C_g concentration on deposit composition	69
Figure 3.23	As plated Cu–P– C_g coating on carbon steel substrate	72
Figure 3.24	(a) SEM and (b) EDX analysis of Cu–P– C_g composite coating	72
Figure 3.25	As plated Cu–P– C_g –SiC coating on carbon steel substrate	74
Figure 3.26	(a) SEM and (b) EDX analysis of Cu–P– C_g –SiC composite coating	74
Figure 3.27	X-ray diffraction patterns of the (a) Cu–P, (b) Cu–P–SiC, (c) Cu–P– C_g and (d) Cu–P– C_g –SiC composite coatings	78
Figure 3.28	DSC thermogram of the (a) Cu–P, (b) Cu–P–SiC, (c) Cu–P– C_g and (d) Cu–P– C_g –SiC composite coatings	83
Figure 3.29	XRD patterns of Cu–P–SiC composite coatings after heat treatment in different temperatures for 1 h	85
Figure 3.30	DSC thermogram of the Cu–P–SiC composite coatings with different SiC concentrations in the bath	86
Figure 3.31	Comparison of the corrosion behaviour of electroless Cu–P–SiC coatings deposited from the baths with	88

different concentrations of SiC in 3.5 % NaCl on carbon steel substrates

Figure 3.32	Comparison of the corrosion behaviour of electroless Cu–P–SiC coatings deposited from the baths with different concentrations of SiC in 1 M HCl on carbon steel substrates	88
Figure 3.33	Comparison of the corrosion behaviour of electroless Cu–P composite coatings in 3.5 % NaCl on carbon steel substrates	90
Figure 3.34	Comparison of the corrosion behaviour of electroless Cu–P composite coatings in 1 M HCl on carbon steel substrates	90
Figure 3.35	Comparison of the corrosion behaviour of Cu–P–SiC coating with Cu–P and carbon steel in NaCl solutions	94
Figure 3.36	Comparison of the corrosion behaviour of Cu–P–SiC coating with Cu–P and carbon steel in HCl solutions	96
Figure 3.37	Polarisation curves of electroless Cu–P–SiC coatings deposited from the baths with different concentrations of SiC in 3.5 % NaCl on carbon steel substrates	98
Figure 3.38	Polarisation curves of electroless Cu–P–SiC coatings deposited from the baths with different concentrations of SiC in 1 M HCl on carbon steel substrates	99
Figure 3.39	Polarisation curves of electroless Cu–P composite coatings in 3.5 % NaCl on carbon steel substrates	102

Figure 3.40	Polarisation curves of electroless Cu-P composite coatings in 1 M HCl on carbon steel substrates	103
Figure 3.41	The SEM images of carbon steel in: (a) 3.5 % NaCl, (b) 1 M HCl solutions	104
Figure 3.42	The SEM images of as plated (a) Cu-P, (b) Cu-P-SiC, (c) Cu-P-C _g and (d) Cu-P-C _g -SiC composite coatings in 3.5 % NaCl solutions	104
Figure 3.43	The SEM images of as plated (a) Cu-P, (b) Cu-P-SiC, (c) Cu-P-C _g and (d) Cu-P-C _g -SiC composite coatings in 1 M HCl solutions	105
Figure 3.44	X-ray diffraction patterns of (a) carbon steel substrates, (b) Cu-P and (c) Cu-P-SiC composite coatings after corrosion processes in 3.5% NaCl solutions	106
Figure 3.45	X-ray diffraction patterns of (a) carbon steel substrates, (b) Cu-P and (c) Cu-P-SiC composite coatings after corrosion processes in 1 M HCl solutions	107
Figure 3.46	Potentiodynamic polarisation curves of as plated electroless Cu-P, Cu-P-SiC coatings and carbon steel in 3.5 %, 10 % and 20 % NaCl solutions	110
Figure 3.47	Comparison of corrosion rate of Cu-P-SiC with Cu-P and carbon steel in NaCl solutions	110
Figure 3.48	Potentiodynamic polarisation curves of as plated electroless Cu-P, Cu-P-SiC coatings and carbon steel in 0.1 M, 0.5 M and 1 M HCl solutions	111

Figure 3.49	Comparison of the corrosion rate of Cu–P–SiC with Cu–P and carbon steel in 0.1 M, 0.5 M and 1 M HCl solutions	112
Figure 3.50	Nyquist plots of electroless Cu–P–SiC composite coatings with different concentrations of SiC and carbon steel in 3.5 % NaCl solution	114
Figure 3.51	Bode plots of electroless Cu–P–SiC composite coatings with different concentrations of SiC and carbon steel in 3.5 % NaCl solution	114
Figure 3.52	Bode phase plots of electroless Cu–P–SiC composite coatings with different concentrations of SiC and carbon steel in 3.5 % NaCl solution	115
Figure. 3.53	Electrochemical equivalent circuits used for fitting the experimental data of electroless Cu–P, Cu–P–SiC coatings and carbon steel in 3.5 % NaCl solution, R_s : solution resistance; CPE: constant phase element; R_{ct} : charge–transfer resistance; R_L : inductance resistance; L: inductance	117
Figure 3.54	Nyquist plots of electroless Cu–P composite coatings and carbon steel in 3.5 % NaCl solution	119
Figure 3.55	Bode plots of electroless Cu–P composite coatings and carbon steel in 3.5 % NaCl solution	120
Figure 3.56	Bode phase plots of electroless Cu–P composite coatings and carbon steel in 3.5 % NaCl solution	120
Figure 3.57	Nyquist plots of electroless Cu–P–SiC composite	124

coatings with different concentrations of SiC in the bath and carbon steel in 1 M HCl solution

Figure 3.58	Bode plots of electroless Cu–P–SiC composite coatings with different concentrations of SiC in the bath and carbon steel in 1 M HCl solution	125
Figure 3.59	Bode phase plots of electroless Cu–P–SiC composite coatings with different concentrations of SiC in the bath and carbon steel in 1 M HCl solution	125
Figure. 3.60	Electrochemical equivalent circuits used for fitting the experimental data of electroless Cu–P, Cu–P–SiC coatings and carbon steel in 1 M HCl solution, R_s : solution resistance; CPE: constant phase element; R_{ct} : charge–transfer resistance	127
Figure 3.61	Nyquist plots of electroless Cu–P composite coatings and carbon steel in 1 M HCl solution	129
Figure 3.62	Bode plots of electroless Cu–P composite coatings and carbon steel in 1 M HCl solution	130
Figure 3.63	Bode phase plots of electroless Cu–P composite coatings and carbon steel in 1 M HCl solution	130
Figure 3.64	The relationship between hardness (HV) and SiC concentration	134
Figure 3.65	The relationship between hardness (HV) and C_g concentration	135
Figure 3.66	The effect of SiC concentration in the bath on wear rate	138

of Cu–P–SiC composite coatings

- Figure 3.67** The effect of C_g content on wear rate of Cu–P– C_g composite coatings 139
- Figure 3.68** SEM micrographs of the cross-sections of the worn surfaces of the composites tested under the load of 1 N: (a) Cu–P, (b) Cu–P–SiC with 4 g L^{-1} SiC, (c) Cu–P–SiC with 5 g L^{-1} SiC, (d) Cu–P–SiC with 6 g L^{-1} SiC, (e) Cu–P– C_g with 3.5 g L^{-1} C_g (f) Cu–P– C_g with 5 g L^{-1} C_g (g) Cu–P– C_g with 6 g L^{-1} C_g and (h) Cu–P– C_g –SiC with 5 g L^{-1} SiC and 5 g L^{-1} C_g 141
- Figure 3.69** Friction coefficient vs. sliding distance for (a) Cu–P, (b) Cu–P–SiC, (c) Cu–P– C_g and (d) Cu–P– C_g –SiC composite coatings 144
- Figure 3.70** Friction coefficient vs. sliding distance for different SiC concentrations in the bath for Cu–P–SiC, composite coatings; (a) 4 g L^{-1} , (b) 5 g L^{-1} and (c) 6 g L^{-1} 146
- Figure 3.71** Friction coefficient vs. sliding distance for different C_g concentrations in the bath for Cu–P– C_g composite coatings; (a) 3.5 g L^{-1} , (b) 5 g L^{-1} and (c) 6 g L^{-1} 148
- Figure 3.72** AFM morphologies of the as plated electroless copper composite coatings: (a) Cu–P, (b) Cu–P–SiC, (c) Cu–P– C_g and Cu–P– C_g –SiC 150

LIST OF SYMBOLS, ABBREVIATIONS AND NOMENCLATURE

Symbols	Descriptions
ABS	Acrylonitrile–butadiene–styrene
AC	Alternating current
AFM	Atomic Force Microscopy
δ_a	Anodic Tafel slope
δ_c	Cathodic Tafel slope
C_g	Graphite
CS	Carbon steel
CTE	Coefficient of thermal expansion
Cu–P	Electroless copper–phosphorous
Cu–P– C_g	Electroless copper–phosphorous reinforced with graphite particles
Cu–P– C_g –SiC	Electroless copper–phosphorous reinforced with silicon carbide and graphite particles
Cu–P–SiC	Electroless copper–phosphorous reinforced with silicon carbide particles
$CuSO_4 \cdot 5H_2O$	Copper sulfate
DSC	Differential Scanning Calorimetry
EC	Electroless copper
EDTA	Ethylenediaminetetraacetic acid
EDX	Energy Dispersive X-ray
EIS	Electrochemical Impedance Spectroscopy
El	Electroless
FC-4	$C_{20}H_{20}F_{23}N_2O_4I$
FD	Freeze drying
H_3BO_3	Boric acid
HTAB	Hexadecyltrimethyl ammonium bromide
I_{corr}	Corrosion current
MEMS	Microelectromechanical system
MMCs	Metal matrix composites
$Na_3C_6H_5O_7$	Sodium citrate

$\text{NaH}_2\text{PO}_2 \cdot \text{H}_2\text{O}$	Sodium hypophosphite
NASP	National aero-space plane
$\text{NiSO}_4 \cdot 6\text{H}_2\text{O}$	Nickel sulfate
OCP	Open circuit potential
Ox	Oxidation
PCB	Printed circuit board
POP	Plating on plastics
PTFE	Polytetrafluoroethylene
R_a	Roughness
RC	Randles cell
R_{ct}	Charge transfer resistance
R.E.	Reference electrode terminal
R_p	Polarisation resistance
R_s	Solution resistance
RT	Room temperature
SCE	Saturated calomel electrode
SEM	Scanning Electron Microscopy
SiC	Silicon carbide
ULSI	Ultra large scale integration
WC	Tungsten carbide
W.E.	Working electrode terminal
W_{Loss}	Weight loss
XRD	X-Ray Diffraction
Z	Impedance

PENYADURAN TANPA ELEKTRIK LITUPAN KOMPOSIT KUPRUM YANG DIPERKUKUHKAN DENGAN ZARAH SILIKON KARBIDA DAN GRAFIT

ABSTRAKT

Dalam kajian ini, litupan komposit Cu-P, Cu-P-SiC, Cu-P-C_g dan Cu-P-C_g-SiC telah diaplikasikan dengan menggunakan kaedah penyaduran tanpa elektrik. Kesan-kesan pH, suhu dan perbezaan kepekatan NaH₂PO₂·H₂O, NiSO₄·6H₂O, silikon karbida (SiC) and grafit (C_g) ke atas kadar penganapan dan komposisi litupan telah dinilai dan formulasi rendaman bagi litupan komposit Cu-P-C_g-SiC telah dioptimumkan. Parameter operasi optimum bagi penganapan Cu-P-C_g-SiC adalah dikenal pasti pada pH 9, suhu pada 90 °C, pada kepekatan masing-masing 125 g L⁻¹ bagi NaH₂PO₂·H₂O, 25 g L⁻¹ bagi CuSO₄·5H₂O, 3.125 g L⁻¹ bagi NiSO₄·6H₂O, 5 g L⁻¹ bagi SiC, 5 g L⁻¹ bagi C_g, 50 g L⁻¹ bagi C₆H₅Na₃O₇·2H₂O dan 25 g L⁻¹ bagi H₃BO₃. Morfologi permukaan litupan yang telah dianalisa menggunakan mikroskop pengimbas elektron (SEM) menunjukkan bahawa taburan zarah Cu adalah seragam dengan beberapa sebatian Si dan zarah C_g. Teknik pembelauan sinar -X (XRD) dan SEM telah digunakan dalam pencirian struktur dan morfologi litupan. Fasa seperti Cu, Cu₂O, Cu₃P, Cu₃Si, SiC dan C_g telah dilihat daripada pola XRD dan kehadiran Cu₂O, Cu₃P dan Cu₃Si telah dipastikan oleh kaedah kalorimeter pembezaan imbasan (DSC). Keputusan telah menunjukkan bahawa SiC dan zarah C_g mempunyai sedikit pengaruh ke atas peralihan fasa litupan. Keputusan yang diperoleh daripada mikroskop tenaga atom (AFM) bagi litupan menunjukkan kekasaran permukaan semakin meningkat dengan penambahan SiC di dalam matriks litupan Cu-P dan berkurangan dengan kehadiran C_g. Litupan komposit Cu-P-C_g-SiC menunjukkan kekasaran yang sederhana diantara kekasaran Cu-P-SiC dan Cu-P-C_g.

Sifat anti-kakisan litupan komposit Cu-P, Cu-P-SiC, Cu-P-C_g dan Cu-P-C_g-SiC di dalam larutan NaCl dan HCl telah dikaji menggunakan kaedah kehilangan berat, polarisasi potensiodinamik dan teknik spektroskopi elektrokimia impedans (EIS). Anjakan nilai keupayaan kakisan (E_{corr}) ke arah lengai, penurunan nilai ketumpatan arus kakisan (i_{corr}), peningkatan rintangan pemindahan cas (R_{ct}) dan penurunan kapasitans lapisan ganda dua (C_{dl}) menunjukkan penambahbaikan dalam rintangan kakisan dengan kehadiran zarah SiC di dalam matriks Cu-P. Kesan kepekatan SiC ke atas rintangan kakisan Cu-P-SiC telah dikaji dan didapati bahawa kesan anti-kakisan terbaik bagi Cu-P-SiC adalah pada kepekatan 5 g L⁻¹ SiC di dalam formulasi rendaman.

Kekerasan dan ketahanan haus bagi litupan komposit Cu-P telah ditingkatkan dengan kehadiran zarah SiC dan peningkatan kepekatan SiC juga meningkatkan kekerasan dan ketahanan haus Cu-P. Pekali geseran bagi litupan komposit Cu-P berkurang dengan kehadiran zarah C_g. Litupan komposit Cu-P-C_g-SiC menunjukkan kekerasan yang sederhana diantara Cu-P-SiC dan Cu-P-C_g, dan geseranyang rendah, anti-haus yang baik dan menunjukkan sifat anti-kakisan.

ELECTROLESS COPPER COMPOSITE COATINGS REINFORCED WITH SILICON CARBIDE AND GRAPHITE PARTICLES

ABSTRACT

In this work, Cu-P, Cu-P-SiC, Cu-P-C_g and Cu-P-C_g-SiC composite coatings were deposited by means of electroless plating. The effects of pH, temperature and different concentrations of NaH₂PO₂·H₂O, NiSO₄·6H₂O, silicon carbide (SiC) and graphite (C_g) on the deposition rate and the coating compositions were evaluated and the bath formulation for the Cu-P-C_g-SiC composite coatings was optimised. The corresponding optimal operating parameters for depositing Cu-P-C_g-SiC were found to be pH 9, temperature at 90 °C, concentrations of NaH₂PO₂·H₂O at 125 g L⁻¹, CuSO₄·5H₂O at 25 g L⁻¹, NiSO₄·6H₂O at 3.125 g L⁻¹, SiC at 5 g L⁻¹, C_g at 5 g L⁻¹, C₆H₅Na₃O₇·2H₂O at 50 g L⁻¹ and H₃BO₃ at 25 g L⁻¹. The surface morphology of the coatings that were analysed using scanning electron microscopy (SEM) showed that Cu particles were uniformly distributed with some Si compounds and C_g particles. X-ray diffraction (XRD) and scanning electron microscopy (SEM) techniques were used to characterise the structure and morphology of the coatings. Phases such as Cu, Cu₂O, Cu₃P, Cu₃Si, SiC and C_g were observed from X-ray diffraction patterns and the presence of Cu₂O, Cu₃P and Cu₃Si was confirmed by differential scanning calorimeter (DSC) studies. The results demonstrated that SiC and C_g particles have little influence on the phase transition of the coating. Atomic force microscopy (AFM) results of coatings showed that the roughness of the coatings increased with the incorporation of SiC to the matrix of Cu-P coatings and decreased with the incorporation of C_g. Cu-P-C_g-SiC composite coatings showed a moderate roughness between Cu-P-SiC and Cu-P-C_g.

The anti-corrosion properties of Cu-P, Cu-P-SiC, Cu-P-C_g and Cu-P-C_g-SiC composite coatings in NaCl and HCl solutions were investigated by the weight loss method, potentiodynamic polarisation and electrochemical impedance spectroscopy (EIS) techniques. The shift in the corrosion potential (E_{corr}) towards the noble direction, decrease in the corrosion current density (i_{corr}), increase in the charge transfer resistance (R_{ct}) and decrease in the double layer capacitance (C_{dl}) values indicated the improvement in corrosion resistance with the incorporation of SiC particles in the Cu-P matrix. The effects of SiC concentrations on the corrosion resistance of Cu-P-SiC were investigated and it was found that the best anti-corrosion of Cu-P-SiC was at 5 g L⁻¹ SiC in the bath formulation.

The hardness and wear resistance of Cu-P composite coatings were improved with the incorporation of SiC particles and with the increase of SiC concentration, the hardness and wear resistance also increased. The friction coefficient of Cu-P composite coatings decreased with the incorporation of C_g particles. Cu-P-C_g-SiC composite coatings showed a moderate hardness between Cu-P-SiC and Cu-P-C_g, and had low friction, good anti-wear and showed some anti-corrosion properties.

CHAPTER ONE

INTRODUCTION AND LITERATURE REVIEW

1.1 Electroless plating

Thin film metallic coatings have been the focus of much interest in recent years. As the cost of metals soars, manufacturers are increasingly turning to more economical means of coating their products. Metal deposition by aqueous solutions can broadly be divided into two categories: electrolytic and electroless. The electroless process supplements and in some cases replaces electrodeposition for several practical reasons. Electroless depositions have excellent throwing power and allow plating on articles with very complex shapes and plating through holes. Deposits obtained by electroless deposition are more dense (more pores-free) and exhibit better properties for corrosion and electronics applications. Other important advantages include its applicability for metallisation of nonconductive surfaces (glass, ceramics, polymers, etc.) and the ability to selectively deposit thin metal films only on catalysed areas of the substrate. Finally, in electroless metal deposition process, no external current supply is required to deposit materials on a substrate. Electroless plating is an autocatalytic process where the substrate develops a potential when it is dipped in an electroless solution called bath, which contains a source metal of metallic ions, reducing agent, stabiliser and others. Due to the developed potential, both positive and negative ions are attracted towards the substrate surface and release their energy through charge transfer process. Each process parameter has its specific role on the process and influences the process response variables. Temperature initiates the reaction mechanism which controls the

ionisation process in the solution and charge transfer process from source to substrate. In addition to this, the substrate is activated before dipping into the electroless bath and sensitised to initiate the charge transfer process (Li, 2003; Oraon *et al.*, 2006).

There are many different processes that can be considered under the heading of nonelectrolytic plating and coating. These include electroless plating (in which a metal compound is reduced to the metallic state by means of a chemical reducing agent in solution), hot dipping, plasma spraying, chemical vapor deposition, diffusion processes, vacuum coating and sputtering. All these different methods have the goal of applying the desired thickness of metal onto a surface in the shortest period of time and at the lowest possible cost (Li, 2003).

Since the discovery of autocatalytic electroless plating by Brenner and Riddel in 1946, its use has continued to grow because of its useful combination of properties and characteristics (Delaunois *et al.*, 2000; Mallory & Hadju, 1990; Oraon *et al.*, 2006). Indeed, electroless plating offers unique deposit properties, including uniformity whatever the substrate geometry. Other features are excellent corrosion, wear and abrasion resistances, good ductility, lubricity, solderability, excellent electrical properties and high hardness (Duffy, 1980).

Surface properties, such as strength and wear resistance of pure copper and carbon steel can be improved by internal oxidation, chemical vapor deposition, electroplating and many other means. However, electroless deposition has the advantages of simplicity and feasibility over other processes. It improves the

adherence between coating and the substrate besides improving properties, like wear resistance (Apachitei & Duszczyk, 2000; Ebrahimian-Hosseinabadi *et al.*, 2006; Sahoo, 2009), hardness (Alirezaei *et al.*, 2004; Tien *et al.*, 2004; Zangeneh-Madar & Monir Vaghefi, 2004), corrosion resistance (Lee *et al.*, 2010; Rabizadeh & Allahkaram, 2011; Tian *et al.*, 2010) and surface roughness (Balaraju *et al.*, 2006a; Huang & Cui, 2007; Yu *et al.*, 2002). The applications of electroless platings have been reported in many industries, such as petroleum, chemical, plastics, optics, aerospace, nuclear, electronic, computer, and printing because of its excellent corrosion and wear resistance properties (Jin *et al.*, 2004; Kumar *et al.*, 2010; Li *et al.*, 2008). Cumbersome wiring and vacuum tubes have been replaced by printed circuits and transistors, and the industry has discovered new and better ways of producing electrically conductive coatings. Better ways of adhering these metals to plastic and ceramic substrates have also received much attention (Duffy, 1980; Mallory & Hadju, 1990). The computer industry has also benefitted from recent advances in the area of magnetic coatings, which are used to produce memory tapes and discs. New processes have produced coatings which are more oxidation-resistant and which can contain a larger amount of information using less space. New processes involving photosensitive coatings are also used in television screens, photographic and photocopy uses. Less traditional application includes solar cell technology (Duffy, 1980; Mallory & Hadju, 1990).

1.2 General process and bath composition

Electroless plating includes general processes which produce deposits without the use of an electric current when all parameters of the bath are correctly maintained (Fig. 1.1-a). Electrons are supplied by a chemical reaction in solution which involves an exchange between two oxido-reduction couples in which one is an oxidising agent and the other a reducing agent according to equation 1.1 (Mallory & Hadju, 1990).

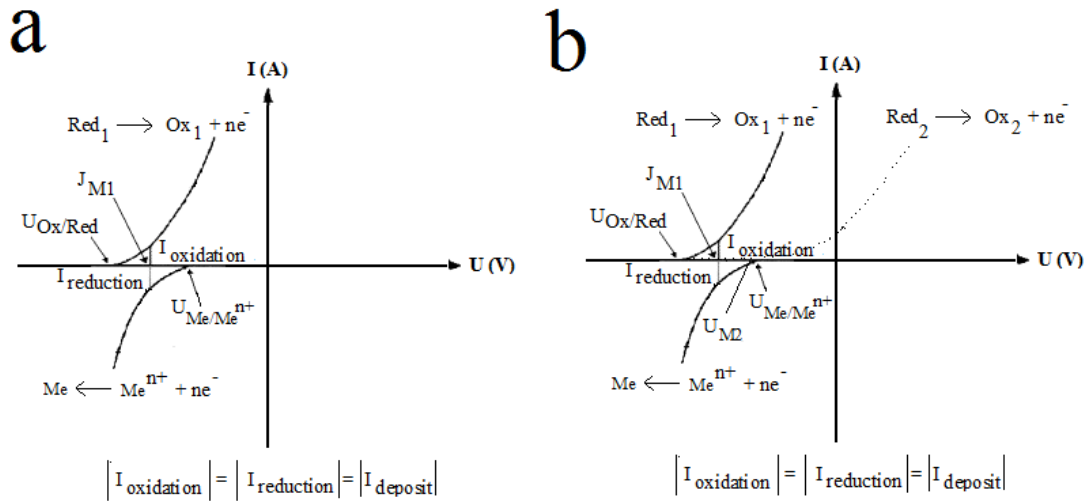


Figure 1.1 Equilibrium established at: (a) mixed potential (b) mixed potential- the catalytic power of metal (Delaunois *et al.*, 2000).

When the reducing agent is present in solution, ready to be oxidised, the process is an electroless reduction. It can lead to non-limited thickness of deposits when the parameters are correctly maintained. The main difficulty of this electroless process is preventing spontaneous metal deposition with solution decomposition (loss of bath stability).

In the case of catalytic deposition, the reduction of the metallic ions in solution is under control and the baths only deposit on metallic substrates. With the addition of complexing agents and stabilisers, the reduction reaction in solution is thermodynamically possible (the potential $U_{\text{Red/Ox}}$ must at least be more negative than the equilibrium potential of the system $U_{\text{Me}^{n+}/\text{Me}}$ (Fig. 1.1-a) but cannot take place due to kinetics which are too slow. The immersion of a catalytic surface breaks this inertia and the reduction reaction can only occur on the immersed catalytic surface. When the deposited metal is also catalytic, the reaction continues by itself and the deposits are described as autocatalytic (Delaunois *et al.*, 2000).

Therefore, with a catalytic support, the anodic oxidation overvoltage of the reducing agent is limited and the mixed potential is shifted to more negative values (Fig. 1.1-b). The oxidation curve of the reducing agent obtained on a non-catalytic metal (Red_2) presents a very low oxidation current up to a value near the current potential $U_{\text{Me}^{n+}/\text{Me}}$. On the other hand, the same curve obtained for a catalytic metal (Red_1) leads to an important oxidation current close to this $U_{\text{Me}^{n+}/\text{Me}}$. A classification of metals was made from galvanostatic tests taking into account their catalytic activity in the presence of different reducing agents (Fig. 1.2), i.e. the potential taken by the metal examined in a solution containing a chosen reducing agent when an anodic current of $10^{-4} \text{ A cm}^{-2}$ is applied. In order for the metal to present catalytic activity with the reducing agent, and that this reducing agent be used for the electroless plating of this metal, the potential $U_{\text{Red/Ox}}$ must at least be more negative than the equilibrium potential of the system $U_{\text{Me}^{n+}/\text{Me}}$ (Fig. 1.1-a). With these considerations, it is possible to choose a series of reducing agents which can be used for electroless deposition. The general composition and the functions of the

components of an electroless bath are given in Table 1.1. These baths are used at high temperatures to obtain a good deposition rate. The principle parameters controlling the composition of coatings from electroless baths are the concentrations of the source metal ion, the complexing agent, stabiliser, buffer, temperature, pH, bath age, bath loading and agitation (Delaunois *et al.*, 2000).

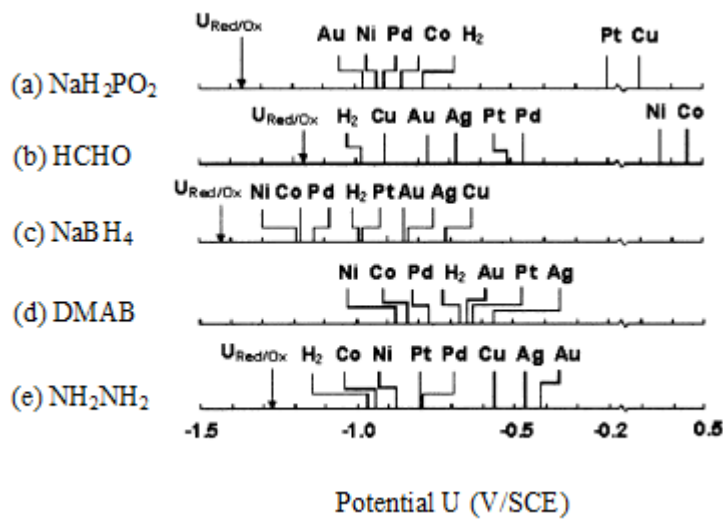


Figure 1.2 Catalytic activities of metals at 25 °C with different reducing agents (Delaunois *et al.*, 2000).

Table 1.1 General electroless bath composition (Delaunois *et al.*, 2000).

Compound	Function
Metallic ions	Supply of metal to be deposited
Reducing agent	Electron source
Complexing agent	Forms a complex with the metal: increases the metallic ion solubility and avoids hydroxides precipitation due to the increase in the stability but the decrease in the deposit current
Stabiliser	Increases the bath stability
Buffer	Increases the pH stability

Some literatures point out that the most important reactions occurring in electroless plating, using chlorides (Ashassi-Sorkhabi *et al.*, 2002; Oraon *et al.*, 2006; Rajendran *et al.*, 2010) and sulphates (Tian *et al.*, 2010; Yan *et al.*, 2008; Zhao & Liu, 2005a) of metallic salts for supplying of metal to be deposited. The following chemicals viz., sodium hypophosphite (NaH_2PO_2) (Amell *et al.*, 2010; Ramalho & Miranda, 2005; Ramalho & Miranda, 2007), dimethylamine borane (DMAB) (Zhu *et al.*, 2004), glyoxylic acid (HCOCOOH) (Sung *et al.*, 2009; Wu & Sha, 2008a; Wu & Sha, 2008b) formaldehyde (HCHO) (Cheng *et al.*, 1997; Ramesh *et al.*, 2009; Sung *et al.*, 2009) and sodium borohydride (NaBH_4) (Oraon *et al.*, 2006; Zhang *et al.*, 2008b) were used as reducing agents.

Sodium citrate ($\text{Na}_3\text{C}_6\text{H}_5\text{O}_7 \cdot 2\text{H}_2\text{O}$) (Gan *et al.*, 2008b; Rudnik & Gorgosz, 2007; Yan *et al.*, 2008), tartrate ($\text{KNaC}_4\text{H}_8\text{O}_6 \cdot 4\text{H}_2\text{O}$) (Cheng *et al.*, 1997), ethylenediaminetetraacetic acid (EDTA) (Mallory & Hadju, 1990) and lactic acid ($\text{CH}_3\text{CHOHCOOH}$) (Amell *et al.*, 2010; Balaraju & Rajam, 2005; Huang *et al.*, 2003; Jiaqiang *et al.*, 2006) were added as a complexing agent while boric acid

(H_3BO_3) (Krishnaveni *et al.*, 2008; Krishnaveni *et al.*, 2005; Rudnik & Gorgosz, 2007), ammonium acetate ($\text{NH}_4\text{CH}_3\text{COO}$) (Zhao & Liu, 2004; Zhao *et al.*, 2004) and sodium acetate ($\text{CH}_3\text{COONa}\cdot\text{H}_2\text{O}$) (Tian *et al.*, 2010) were used as buffer.

Thiourea (Huang *et al.*, 2003; Zhang *et al.*, 2008b), $(\text{CH}_2)\text{CS}$ (Liu & Zhao, 2004; Zhao & Liu, 2005a; Zhao *et al.*, 2004) and maleic acid ($\text{C}_4\text{H}_4\text{O}_4$) (Rudnik & Gorgosz, 2007; Rudnik *et al.*, 2008) were added as stabilisers whereas polyglycol (Liu *et al.*, 2007a), hexadecyltrimethyl ammonium bromide (HTAB) (Wu *et al.*, 2006a; Wu *et al.*, 2006b; Wu *et al.*, 2006c) and $\text{C}_{20}\text{H}_{20}\text{F}_{23}\text{N}_2\text{O}_4\text{I}$ (FC-4) (Tian *et al.*, 2010; Zhao & Liu, 2004; Zhao *et al.*, 2004) were used as surfactants.

1.3 Electroless copper (EC) and functional applications

Electroless copper chemistry was first reported in the mid-1950s with the developments of plating solutions plated through-hole (PTH) for printed wiring boards (Sharma *et al.*, 2006).

Diversified metallic and nonmetallic surfaces endowed with attractive appearance, high corrosion resistance, electromagnetism low density, and some other special functions were produced by electroless copper (EC). The EC technique is a cost-effective and is a widely used electrochemical process for the deposition of Cu films. It has been widely used in the electronic industry, machinery manufacturing and National Aero-Space Plane (NASP) airframe because of its excellent thermal conductivity (Guo *et al.*, 2009; Han *et al.*, 2010; Hwang *et al.*, 2009; Li, 2003).

In view of the ease with which it may be deposited itself and electroplated with other metals, copper is particularly useful as a pre-coating for soft soldered work, pewter and zinc alloy diecastings before the deposition of Ni, gold, silver, etc. Another large scale use of copper plating is in the electronics industry where, because of its conductivity, it is used to produce the millions of square feet of printed circuit boards each year (Li, 2003; Mallory & Hadju, 1990).

Copper is plated on to slowly revolving stainless steel drums and because there is no adhesion it can be peeled off in a continuous manner to be subsequently bonded to epoxy resin or phenolic sheets. When this material has been cut up, drilled and suitable circuit patterns defined on the surface, copper plating is again used as part of the through-hole plating technique (Mallory & Hadju, 1990). With the recurrent shortage of Ni, considerable attention has been paid to the possibility of using electrodeposited Cu as a partial or complete replacement for plating (Li, 2003).

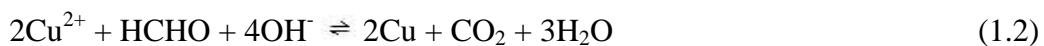
An interesting application of Cu plating is in connection with the selective case hardening of steel. The Cu deposit is applied or retained on those areas which are to remain unhardened, and its presence prevents penetration by the carbon during the subsequent carburizing process. Selective case hardening is now applied to a wide range of engineering components which are subjected to wear, including gears, spline shafts, motor and aircraft fillings. Through the use of this technique the actual wearing surfaces are made extremely hard while the remaining surface of the component is soft enough to permit further machining. A further advantage to be gained from the use of selective case hardening is that by restricting the area of the

component which is hardened, the loss in fatigue strength in the material is greatly reduced (Li, 2003).

In the printing industry copper is used for the production of electrotypes and for providing the printing surface in gravure printing. Copper is used in electroforming for the production of wave guides and other electrical and electronic hardware. The metal has also found use in the production of electroformed slush moulds for rubber and plastic items and is employed as a back-up material for the harder nickel electroforms used in pressure moulds (Li, 2003).

Other occasional uses are in the building up of surfaces where mechanical loading is not too high, and for the plating of wire to act as a lubricant prior to drawing. Carbon brushes and arc electrodes are sometimes copper plated in order to improve their electrical conductivity. Copper plating is also useful for providing an anti-fret coating on bearings and housing (Li, 2003; Mallory & Hadju, 1990).

Conventional EC plating baths usually use formaldehyde (HCHO) as the reducing agent (Ramesh *et al.*, 2009; Vaskelis *et al.*, 2007) which is carcinogenic in nature. This technique was operated at pH values above 11 (Cheng *et al.*, 1997):



the Cannizzaro reaction:



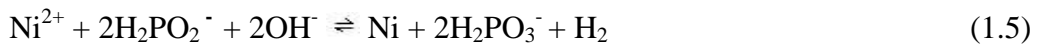
and the carbonation reaction 1.3:



Fluctuations in component concentration and bath temperatures are inherent and unavoidable in the course of commercial use of the bath and these are normally detrimental to protracted use of formaldehyde-reduced copper solutions. The bath stability is maintained better, in spite of these inherent fluctuations by using sodium hypophosphite as a reducing agent.

Therefore, sodium hypophosphite that has been used to replace formaldehyde is especially attractive because of its low pH, low cost, and relatively safe features compared with high pH formaldehyde-based solutions (Afzali *et al.*, 2010; Cheng *et al.*, 1997; Gan *et al.*, 2007b; Gan *et al.*, 2008b). However, Cheng *et al.* (1997) reported that the catalytic activities of metals for the oxidation of hypophosphite decreased in the following order: Au > Ni > Pd > Co > Pt > Cu; thus, the reaction of EC deposition in hypophosphite-type baths was impossible without a catalyst. Therefore Ni²⁺ ions are used as catalysts for the EC deposition. The reactions of Ni as a catalyst are as follows:

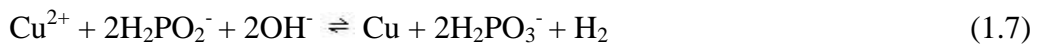
Nickel deposition reaction



Replacement reaction

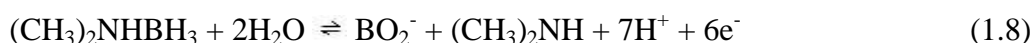


Adding Eq. 1.3 and 1.4,



It can be seen that Ni²⁺ ions do not appear in reaction 1.7 and that nickel only plays the role of a catalyst for the hypophosphite oxidation (Cheng *et al.*, 1997).

Although dimethylamine borane (DMAB) is not widely used in the electroless plating of metals due to the high cost, its good reduction ability provides the convenience for controlling the deposition rate at an ideal level. The special electroless bath solutions were prepared with DMAB as a reducing agent and sodium citrate ($\text{Na}_3\text{C}_6\text{H}_5\text{O}_7$) as a complexing agent to trigger the formation of nano-sized copper particles in the solution by Zhu *et al.* (2004). No catalyst was employed and the half reaction is as follows:



1.4 Carbon steel (CS)

Most large metal structures are made from carbon steel-the world's most useful structural material. Carbon steel is inexpensive, readily available in a variety of forms, and can be machined, welded, and formed into many shapes. Carbon steel is widely used in the fabrication of reaction vessels, store tanks and petroleum refineries (Noor & Al-Moubaraki, 2008; Quraishi *et al.*, 2003). Carbon steel has been widely employed as a construction material for pipe work in the oil and gas production, such as down hole tubulars, flow lines and transmission pipelines. However, one of the major problems related to its use is its low corrosion resistance in these environments. For example, one of the largest problems in operating pipe flow lines is their internal corrosion. This kind of corrosion depends mainly on the composition of the oil. Carbon dioxide (CO_2) corrosion, which is commonly called sweet corrosion, is one of the most serious forms of corrosion in the oil and gas production and transport industry (Ghareba & Omanovic, 2010). CO_2 is normally present in deep natural gas reservoirs and it could be present in the oil due to its injection to the reservoir to force the oil to flow out more easily for enhanced oil

recovery (Jiang *et al.*, 2006). Sweet corrosion failures have been reported to account for some 25 % of all safety-related incidents (Bayliss & Deacon, 2002). Corrosion behaviour of steels is very important and mainly investigated in inorganic acids (Arslan *et al.*, 2009; Behpour *et al.*, 2008; Quraishi *et al.*, 2010), salts (Ai *et al.*, 2006; Al-Refaie *et al.*, 2010; Amar *et al.*, 2008), non-oxidation organic acids (Nagies & Heusler, 1998; Wang *et al.*, 2001), alkaline solutions (Abd El Haleem *et al.*, 2010; Macías & Escudero, 1994; Singh *et al.*, 2002), and marine media (Melchers, 2008; Meng *et al.*, 2007; Wan *et al.*, 2010).

Several methods are present for corrosion prevention of carbon steel. One such method is the use of an organic (Bentiss *et al.*, 2002; Lagrenée *et al.*, 2002; Sathiyarayanan *et al.*, 2005) or inorganic (Oguzie, 2004; Refaey *et al.*, 2000; Umoren *et al.*, 2008) inhibitors. Because of their aggressiveness, inhibitors are used to reduce the rate of dissolution of metals. Compounds containing nitrogen, sulphur and oxygen are being used for this purpose (Bothi Raja & Sethuraman, 2008; Rahim *et al.*, 2008; Rahim *et al.*, 2007; Sastry, 1998).

Conducting polymers as either film forming corrosion inhibitors or in protective coating have attracted more and more attention due to the excellent anti-corrosion ability and environmental friendliness. Several studies have been carried out and reported on the protective behaviour of conducting and insulating forms of polymers on steel. Conducting polymer coatings such as polyaniline (PAni) (Benchikh *et al.*, 2009; Sathiyarayanan *et al.*, 2010; Yao *et al.*, 2008) and polypyrrole (Ferreira *et al.*, 1996; Herrasti & Ocón, 2001; Hosseini *et al.*, 2007) on steel electrodes can be obtained electrochemically and these coatings provide

important protective properties against corrosion. Conducting polymer coatings on steel surface also inhibit the formation of pitting corrosion in chloride medium.

1.5 Composite coating

The development of ‘clean’ technologies in all spheres of industrial manufacturing is today an essential task and initiated by environmental laws and programmes of countries around the world. Among the major sources of environmental pollution are technologies and processes used in conventional metal finishing operations such as electroless and electroplating of protective functional and decorative coatings (Navinsek *et al.*, 1999).

Electroless plating is one of the methods by which composite coatings can be produced. It is well known that electroless metal coating has a high plating capability, high bonding strength, excellent weldability, electrical conductivity, good antiwear and controllable magnetic properties through suitable heat treatment (Hu *et al.*, 2003).

In the chemical, petrochemical, metallurgical and marine industrial environments, many mechanical components often work in environments which are subjected to the simultaneous action of mechanical wear and chemical attack, and thus are always liable to the premature failure of materials (De Las Heras *et al.*, 2008; Smith *et al.*, 2006). The phenomenon is usually initiated by synergistic effects of electrochemical corrosion and mechanical erosion, which result in a greater rate of materials damages than the sum of the individual contribution of wear and corrosion (Malka *et al.*, 2007). Because of a lack of a combination of wear and corrosion

properties, the traditional corrosion or wear-resistance engineering materials, such as stainless steels and alloy tool steels, are hard to be applied in those environments. Consequently, the optimisation of the balance between mechanical erosion and corrosion resistance to achieve the least synergism is an appropriate way to reduce mass loss of materials exposed to erosion–corrosion environment. Furthermore, the mechanical and tribological properties of metal coatings can be improved by the incorporation of different solid particles which are categorised as hard such as: silicon carbide (SiC) (Apachitei *et al.*, 2001; Chen *et al.*, 2002; Gou *et al.*, 2010; Lin & He, 2006; Liu *et al.*, 2007b; Yuan *et al.*, 2009; Zoikis-Karathanasis *et al.*, 2010), aluminium oxide (Al₂O₃) (Balaraju *et al.*, 2006b; Tian & Cheng, 2007), titanium oxide (TiO₂) (Chen *et al.*, 2010; Novakovic *et al.*, 2006; Shibli & Dilimon, 2007; Zhang *et al.*, 2010), zirconium oxide (ZrO₂) (Gay *et al.*, 2007; Szczygiel & Turkiewicz, 2009; Szczygiel *et al.*, 2008), boron carbide (B₄C) (Ebrahimian-Hosseini *et al.*, 2006), tungsten carbide (WC) (Hamid *et al.*, 2007) and diamond (Sheela & Pushpavanam, 2002) to enhance the hardness and/or wear resistance of the deposits, or can be dry lubricants such as: graphite (C_g), molybdenum disulfide (MoS₂) (Moonir-Vaghefi *et al.*, 1997a; Moonir-Vaghefi *et al.*, 1997b) and polytetrafluoroethylene (PTFE) (Zhao *et al.*, 2002) to impart lubricity and reduce the coefficient of friction.

In recent years, electroless plating has won great popularity in preparing composite coatings, which are generally prepared by adding solid particles to the regular electroless plating solution to achieve co-deposition of the solid particles and matrix (Araghi & Paydar, 2010; Balaraju *et al.*, 2010; Chen *et al.*, 2010; León *et al.*, 2006). Among the solid particles used for reinforcement, SiC is most frequently

studied and applied. SiC particles are of great technological importance for their applications as semiconductor materials and structural ceramics and have high material strength with excellent corrosion, erosion resistance, thermal conductivity and mechanical and physical properties (Grosjean *et al.*, 2001; Pelleg *et al.*, 1996). In recent years, SiC has found new applications in the electronic industry for its excellent and adjustable dielectric properties (Zhao *et al.*, 2008). With the electroless plating process, solid SiC particles used for reinforcements are added to the plating solution and are stirred to avoid sedimentation of particles in the solution so that co-deposition of the discrete SiC particles can be obtained (Zhang *et al.*, 2008a). Consequently, corrosion resistance (Yuan *et al.*, 2009), the micro-hardness and wear resistance (Apachitei *et al.*, 2002; Grosjean *et al.*, 2001; Liu *et al.*, 2007b) of composite coatings is greatly improved with incorporation of SiC particles.

In joining metals to ceramics one major problem is the considerable difference in coefficient of thermal expansion (CTE) between the generally low CTE ceramic and the higher CTE metal. One possible solution to this problem is the use of ductile metal interlayers to accommodate differential thermal strain. Copper is one such potential interlayer material (Qin & Derby, 1991). In particular one can find applications for SiC in many different areas, such as coatings against corrosion covering fuel particles used in a high-temperature gas-cooled reactors, protective layers to be used at high temperatures, or corrosion resistant coatings in biological media on metal implants (Ordine *et al.*, 2000). The interactions between SiC and Cu have been investigated by some authors (Lee & Lee, 1992; Nikolopoulos *et al.*, 1992; Qin & Derby, 1991; Wang & Wynblatt, 1998).

1.5.1 Reinforcement of coatings by silicon carbide

SiC also known as *carborundum*, is a compound of silicon and carbon. It occurs in nature as the extremely rare mineral moissanite. Silicon carbide powder has been mass-produced since 1893 for use as an abrasive. Grains of silicon carbide can be bonded together by sintering to form very hard ceramics which are widely used in applications requiring high endurance, such as car brakes and ceramic plates in bulletproof vests. Electronic applications of silicon carbide as light emitting diodes and detectors in early radios were first demonstrated around 1907, and nowadays SiC is widely used in high-temperature/high-voltage semiconductor electronics. Silicon carbide with a high surface area can be produced from SiO₂ contained in plant materials (Bansal, 2005; Harris, 1995). Silicon carbide is a covalent ceramic of great technological interest because of its good mechanical properties, high thermal conductivity, good thermal shock behaviour and high oxidation resistance. It is especially used as a structural material in high temperature applications or as reinforcement in metal matrix composites. Metal/ceramic interface properties are very important for these applications, i.e. for metal/ceramic and ceramic/ceramic joining by brazing alloys or for infiltration of ceramic fibres by liquid metals or alloys (Bansal, 2005). Generally good wetting (Rado *et al.*, 2000; Rado *et al.*, 1999) and low reactivity (Rado *et al.*, 2000) are required, in order to facilitate fabrication processes, to avoid degradation of ceramics by excessive bulk reactivity and to achieve the desired properties during service.

Co-deposits consist of solid particles incorporated in a metallic matrix are made in order to obtain the properties of the metal and particles. A composite is a multiphase solid in which two or several components are associated in order to obtain a macroscopic scale with completely new set of properties. The particles increase its mechanical, physical properties (Alirezai *et al.*, 2004; León *et al.*, 2005) and corrosion resistance (Balaraju *et al.*, 2006b).

Apachitei and Duszcyk (2000) have reported that the properties of the NiP matrix depend in general on the phosphorus content and temperature. Phosphorus content is essential in establishing the structure of the NiP matrix. In the as-deposited state, the NiP matrix is nanocrystalline with supersaturated solid solution of phosphorus in nickel at low phosphorus contents (e.g. 1–6 wt. % P), or can exhibit an amorphous structure at high concentrations of the alloying element (e.g. 8–12 wt.% P). A transition structure where both types of phases coexist (small crystallites embedded in an amorphous matrix) can be expected for medium-phosphorus contents. Apachitei *et al.* (2001) have also investigated the influence on the structure of the as deposited NiP matrix with the incorporation of SiC particles and showed the formation of nickel silicides at the SiC/matrix interface at lower temperatures (i.e. 500 °C for 1 h). The formation of silicides appeared to be governed by the diffusion of nickel atoms into the SiC lattice, as indicated by transmission electron microscopy. Electroless Ni–P coatings containing SiC particles have been co-deposited on SKD61 tool steel substrate and the effect of heat treatment on the microstructure of Ni–P–SiC composite coatings have been investigated by Chen *et al.* (2002).

The study of the mechanical (hardness) and tribological (friction resistance and wear) properties of the Ni–P–SiC composite coatings have been studied by Grosjean *et al.* (2001). The results show that increasing the size or the rate of SiC particles incorporated lead to an increase in both the hardness of the films and friction coefficient due to their abrasive properties when sliding against a steel ball.

Jiaqiang *et al.* (2006) have shown that SiC particles with three sizes of superfine particles co-deposited homogeneously, and the structure of Ni–P–SiC composite coatings as deposited was amorphous. After certain heat treatment, the matrix of composite coatings crystallised into nickel crystal and nickel phosphide (Ni₃P). At the higher temperature nickel reacted with SiC, and nickel silicides with free carbon were produced. The reaction temperature in electroless composites coatings decreased with the decrease in the size of SiC particles.

Among many other possible technological applications SiC is an interesting material to be used as a protective coating to improve the lifetime or the performance of metallic substrates when exposed to aggressive environments. One acceptable explanation for these good properties could be the very strong covalent bonding between silicon and carbon and its tetrahedral coordination. However, it is well known that two main requirements must be fulfilled in order to achieve a remarkable effect by a protective layer. These are a strong adhesion to the substrate and a low density of pores and cracks (Ordine *et al.*, 2000).

The effect of SiC content on the corrosion resistance of Ni–P–SiC composite coatings immersed in different corrosive solutions (i.e. 5 % H₂SO₄, 20 % NaOH and 3.5% NaCl) have been investigated by Zhang *et al.* (2008). Corrosion tests indicate that in NaOH solution there is no difference in the corrosion resistance between Ni-P coatings and electroless Ni–P–SiC composite coatings, both being uncorroded. Exposed to NaCl solution, the corrosion resistance of electroless Ni–P–SiC composite coatings decreases gradually with the increasing of SiC content in coatings. In H₂SO₄ solution, the corrosion resistance of coatings increases initially and decreases afterwards with the sustained increasing of SiC content in coatings, and the optimised corrosion resistance is obtained at a SiC content of 9.41 wt. %.

Electroless deposition of nickel and cobalt from alkaline baths as well as their codeposition with SiC particles have been compared by Rudnik *et al.* (2008). It has been found that despite similarities in properties of the metals, the electroless process behaviour was different. The favoured deposition of the Co–P/SiC composites was associated probably with less adsorption of the OH[−] ions on the carbide surface in the cobalt bath in comparison with the nickel solution. It has also been reported that Cu-SiC composites have been used as a heat sink material for fusion applications owing to the high-thermal conductivity of Cu and the low swelling of SiC ceramic under neutron irradiation (Gan *et al.*, 2008a). Furthermore, copper and copper-based alloys are widely used in the electrical industry. The addition of ceramic reinforcements such as alumina, silicon carbide and cerium oxide to form metal matrix composites (MMCs) enhances the properties such as elastic modulus, higher strength, better wear resistance, higher coefficient of friction and high-temperature durability. These attractive properties are expected to widen the applications of

copper composite materials compared to copper (Cros *et al.*, 1990; Ramesh *et al.*, 2009; Shu & Tu, 2001). However, the coating hardness is correspondingly decreased with the volume fraction of lubricating particles in the coating and the friction coefficient become worse because of the hard particles.

To solve the above problem, complex composite coatings containing both hard and lubricating particles like C_g (Guo & Tsao, 2000; Wu *et al.*, 2006b; Wu *et al.*, 2006c) and PTFE (Huang *et al.*, 2003; Losiewicz *et al.*, 1999; Straffelini *et al.*, 1999; Zhao & Liu, 2005b; Zhao *et al.*, 2004) are receiving more and more attention.

1.5.2 Reinforcement of coatings by graphite (C_g)

It is known that graphite is one of the frequently used solid lubricant materials just like PTFE and has some advantages over PTFE in the aspects of electrical conductivity and anti high temperature. Additionally, graphite can keep friction coefficient constant under high temperature and high sliding velocity because of its insensitiveness to temperature (Zhang & Zhou, 1993).

Straffelini *et al.* (1999) studied the tribological behaviour of Ni–P–PTFE–SiC composite coating, while Huang *et al.* (2003) discussed the microstructure and properties of Ni–P–PTFE–SiC. Additionally, Losiewicz *et al.* (1999) reported the phase composition and surface morphology of an electrolytic Ni–P–TiO₂–PTFE composites for an electrochemical reaction electrode. Ted Guo and Tsao (2000) introduced the tribological behaviour of aluminium/SiC/nickel-coated graphite hybrid composite synthesised by the semi-solid powder densification method. Wu *et al.* (2006) investigated the tribological behaviour of electroless Ni–P–C_g–SiC.

According to these authors, it is well known that the electroless Ni–P composite coating has good hardness and antiwear with the incorporation of hard particles (like SiC and TiO₂) and friction coefficient of coatings improves with the incorporation of solid lubricant materials (like C_g and PTFE).

1.6 Corrosion

1.6.1 Fundamentals

Corrosion can be defined as the degradation of a material due to a reaction with its environment. Degradation implies deterioration of physical properties of the material. This can be a weakening of the material due to a loss of cross-sectional area, it can be the shattering of a metal due to hydrogen embrittlement, or it can be the cracking of a polymer due to sunlight exposure. Materials can be metals, polymers (plastics, rubbers, etc.), ceramics (concrete, brick, etc.) or composites-mechanical mixtures of two or more materials with different properties. Most corrosion of metals is electrochemical in nature (Baboian, 1986; Uhlig & Winston Revie, 1985).

1.6.2 Why metals corrode

Metals undergo corrosion because they are chemically unstable in the environment. Only precious metals (gold, silver, platinum, etc.) are found in nature in their metallic state. All other metals, including iron-the metal most commonly used are processed from minerals or ores into metals which are inherently unstable in their environments. All other metals are unstable and have a tendency to revert to their more stable mineral forms. Some metals form protective oxides films (passive

films) on their surfaces and these prevent, or slow down, their corrosion process (Bayliss & Deacon, 2002; Landolt, 2007; Uhlig & Winston Revie, 1985).

1.6.3 Corrosion measurements

Since corrosion is an electrochemical process, it follows that electrochemical techniques and electrochemical instrumentation can be used to study the corrosion process. Indeed, a number of electrochemical techniques have been developed over the years especially for the measurement of corrosion processes. Electrochemical techniques are very well accepted by the corrosion community. The reasons for the popularity of electrochemical techniques for corrosion measurement are based on practicality (Baboian, 1986; Uhlig & Winston Revie, 1985):

1. They are fast. Corrosion, even rapid corrosion, is a slow process. Real-time weight loss measurements need days and sometimes weeks to make a reliable measurement of corrosion rate. Electrochemical instrumentation can make a corrosion rate measurement in minutes or hours.
2. They are sensitive. Modern, well-designed electrochemical instrumentation can measure extremely low corrosion rates.
3. They are accurate. Electrochemical techniques have been exhaustively tested before finding general acceptance.
4. They are versatile. Electrochemical techniques can be used to study a wide range of corrosion-related phenomena. The rate of uniform corrosion can be measured. The tendency of a metal to exhibit localized (pitting or crevice) corrosion can be measured. The passivation behaviour of a corroding system can be studied. Galvanic corrosion can be quantitated. Sensitisation effects can be studied. Electrochemistry

can be used in the laboratory or outdoors. Measurements can be made on the lab bench or in a pipeline or in an autoclave or in a slow strain rate machine.

Since electrochemistry was recognised many years ago as the basis for corrosion, a number of electrochemical techniques have been developed specifically for corrosion measurements. These are generally referred to as "DC (direct current) Techniques". Among these techniques are polarisation resistance, Tafel Plots, potentiodynamic plots and cyclic polarisation (Baboian, 1986; Jones, 1995).

1.6.3.1 Potentiodynamic polarisation

Nearly all metal corrosion occurs via electrochemical reactions at the interface between the metal and an electrolyte solution. A thin film of moisture on a metal surface forms the electrolyte for atmospheric corrosion. Wet concrete is the electrolyte for reinforcing rod corrosion in bridges. Although most corrosion takes place in water, corrosion in non-aqueous systems is not unknown. Corrosion normally occurs at a rate determined by an equilibrium between opposing electrochemical reactions. The first is the anodic reaction, in which a metal is oxidised, releasing electrons into the metal. The other is the cathodic reaction, in which a solution species (often O_2 or H^+) is reduced, removing electrons from the metal. When these two reactions are in equilibrium, the flow of electrons from each reaction is balanced, and no net electron flow (electronic current) occurs. The two reactions can take place on one metal or on two dissimilar metals (or metal sites) that are electrically connected. The equilibrium potential assumed by the metal in the absence of electrical connections to the metal is called the open circuit potential, E_{oc} .

The value of either the anodic or cathodic current at E_{oc} is called the corrosion current, I_{corr} . If we could measure I_{corr} , we could use it to calculate the corrosion rate of the metal. Unfortunately I_{corr} cannot be measured directly. However, it can be estimated using electrochemical techniques. In any real system I_{corr} and corrosion rates are a function of many system variables including type of metal, solution composition, temperature, solution movement, metal history, and many others. The above description of the corrosion process does not say anything about the state of the metal surface. In practice, many metals form an oxide layer on their surface as they corrode. If the oxide layer inhibits further corrosion, the metal is said to passivate. In some cases, local areas of the passive film break down allowing significant metal corrosion to occur in a small area. This phenomena is called pitting corrosion, or simply pitting. Because corrosion occurs via electrochemical reactions, electrochemical techniques are ideal for the study of the corrosion processes. In electrochemical studies a metal sample a few cm^2 in surface area is used to model the metal in a corroding system. The metal sample is immersed in a solution typical of the metal's environment in the system being studied. A conventional three electrode cell with carbon steel, saturated calomel electrode and Pt wire as the working, reference and counter electrode, respectively is used to carry out the potentiodynamic polarisation studies. A potentiostat allows you to change the potential of the metal sample in a controlled manner (Baboian, 1986).

The Tafel calculation is an ideal tool to determine the corrosion rate at a metal sample surface. When the linearity range of the $\log(i) = f(E)$ curve covers more than one current decade of the cathodic branch and around one decade of the